Macromolecules 1989, 22, 2482-2486

Phase Diagrams for Binary Polymer Systems Exhibiting both Crystallization and Limited Liquid–Liquid Miscibility

W. R. Burghardt

Department of Chemical Engineering, Stanford University, Stanford, California 94305.

Received August 8, 1988; Revised Manuscript Received October 14, 1988

ABSTRACT: Equilibrium phase diagrams have been calculated for binary polymer solutions and blends exhibiting both crystallinity and limited liquid–liquid miscibility, using Flory–Huggins solution thermodynamics. The interaction of crystallization and liquid demixing results in a monotectic phase structure. Phase diagrams calculated for polymer solutions agree well with published experimental observations, such as small shifts in the crystal melting curve despite large variations in the solvent quality. Consideration of the free energy of mixing curve indicates that liquid–liquid phase separation may play a role in determining crystal morphology, even when there is no liquid–liquid equilibrium in the phase diagram. A phase diagram incorporating both monotectic and eutectic phase structures may result from a solution of polymer in a high-melting poor solvent. Phase diagrams calculated for immiscible binary blends indicate only negligible melting point depression over most of the composition range.

Introduction

The properties of polymeric materials are inherently dependent on their microscopic morphology, which in turn is a strong function of their processing history. In many cases, phase separation phenomena play a major role in controlling the morphology of polymer products. For example, polymer blends of commercial importance are often immiscible,[1] and details of the multiphase morphology have a large impact on mechanical properties such as impact strength. Even in single-component systems, control of phase separation during processing allows for products with extremely useful properties. An excellent example of this is given by the asymmetric ultrafiltration or reverse osmosis membrane.[2] Thus, a major goal of research in polymer science has been to understand phase separation phenomena in polymers.

In general, two sorts of phase separation are present in polymer systems (neglecting more complicated materials such as block copolymers): liquid–liquid demixing and crystallization. An important first step in analyzing polymer phase behavior is the calculation of equilibrium phase diagrams. Liquid–liquid phase diagrams have been calculated for a variety of solution models,[1,3,4] while the analysis of equilibrium crystal saturation curves has also received much attention.[5] In many cases, however, both crystallization and liquid demixing are possible. Early work on polymer solution crystallization demonstrated both kinds of phase separation occurred in poor solvents, either by direct observation of the various phases[6,7] or by the invariance of the crystal melting point over a certain concentration range, indicating the presence of two liquid phases in consequence of the phase rule.[8,9] Nakajima and co-workers later observed such phase behavior in polyethylene[10] and isotactic polypropylene[11] solutions in a wide variety of solvents.

In addition to these older studies, several recent papers have also dealt with phase separation in these more complicated systems. Schaaf et al. have studied the unique morphologies that result from crystallization from polymer solutions with limited liquid–liquid miscibility,[12] while the structures resulting from spinodal decomposition and crystallization in binary polymer blends have been investigated by Tanaka and Nishi[13] and by Inaba and coworkers.[14,15] In both solutions and blends, it is seen that the combination of crystallization and liquid–liquid demixing offers greater flexibility in controlling the microscopic morphology of polymeric systems by phase separation. Although the qualitative nature of phase diagrams that include both crystallization and liquid–liquid phase separation is well understood,[3,5] given this renewed interest it is surprising that such phase diagrams have not yet been explicitly calculated, with the exception of one study for a *ternary* polymer–solvent–nonsolvent system.[16] The purpose of this paper is therefore to present calculated phase diagrams for a variety of model binary polymeric systems in which both crystallization and limited liquid–liquid miscibility are taken into account. Such phase diagrams serve a vital function in providing a formal basis for discussion of observed phenomena, as well as for predicting new phenomena in these systems.

Theory

The calculation of equilibrium phase diagrams requires expressions for the chemical potentials of all species in all phases. For liquid phases, this first requires an expression for the free energy of mixing based upon some solution model. In this paper, it is assumed that the Flory–Huggins lattice treatment is an adequate approximation.[3] The condition for equilibrium between two liquid phases A and B is

$$\Delta\mu_i^{\mathrm{A}} = \Delta\mu_i^{\mathrm{B}} \quad (i = 1, 2) \tag{1}$$

The locus of solutions to eq 1 as χ varies with temperature constitutes the binodal curve.

Equilibrium between a crystalline polymer and a polymer solution requires

$$\Delta\mu_2^{\mathrm{L}} = \Delta\mu_2^{\mathrm{C}} \tag{2}$$

where superscript C denotes the crystalline phase and L denotes a liquid phase. $\Delta\mu_2^{\mathrm{C}}$ may be given as a function of temperature following the usual arguments,[3] and the chemical potential for liquid phases is evaluated by using the Flory–Huggins solution model;[1,3] when these expressions are substituted into eq 2, the relations

$$\frac{1}{T_{\mathrm{m}}} = \left[1 + \frac{R\beta}{\Delta H_{\mathrm{u}}}(1 - \Phi_2)^2\right]^{-1}\left[\frac{1}{T_{\mathrm{m}}^{0}} + \frac{R}{\Delta H_{\mathrm{u}}}\left[\left(1 - \frac{1}{r}\right)(1 - \Phi_2) - \frac{\ln \Phi_2}{r} - \alpha(1 - \Phi_2)^2\right]\right] \tag{3a}$$

$$\frac{1}{T_{\mathrm{m}}} = \frac{1}{T_{\mathrm{m}}^{0}} - \frac{R}{\Delta H_{\mathrm{u}}}\left[\frac{\ln \Phi_2}{r} + \chi(T_{\mathrm{m}})(1 - \Phi_2)^2\right] \tag{3b}$$

result for the polymer melting temperature of polymer with degree of polymerization r in solution (a) or in a symmetric blend (b), in which both components have the same molar

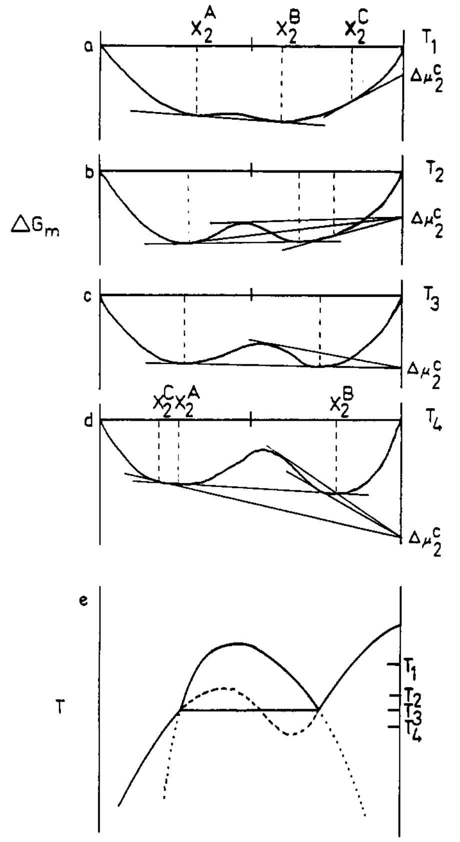

Figure 1. Free energy of mixing vs composition curves at a variety of temperatures (a–d) and the resulting phase diagram (e).

volume. In eq 3a, it is assumed that the interaction parameter has temperature dependence $\chi(T) = \alpha + \beta/T$, as is often the case for polymer solutions,[3] while the temperature dependence of χ has been left implicit in eq 3b. ΔH_u is the enthalpy of fusion per repeat unit, and it is assumed that the molar volumes of the polymer repeat units and the solvent molecules are the same.

When a liquid–liquid two-phase region exists, $\Delta\mu_2^L$ is necessarily multivalued as a function of composition, so that eq 2 has multiple solutions. This is best discussed in terms of a free energy of mixing vs concentration diagram, as given in Figure 1. For temperatures below T_m^0, pure polymer can exist in a crystalline phase, denoted as $\Delta\mu_2^C$, with lower free energy than the corresponding liquid. Following the well-known geometrical construction, the intercept of the local tangent to the ΔG_m vs x_2 curve on the pure polymer axis is simply $\Delta\mu_2^L$. Thus, as shown in Figure 1a, the equilibrium in eq 2 is satisfied by the tangent connecting the point at x_2^C with the polymer crystal, while liquid–liquid equilibrium between phases of composition x_2^A and x_2^B according to eq 1 is also shown. As the temperature is lowered in Figure 1b–d, $\Delta\mu_2^C$ becomes lower, and it is possible to construct as many as three solutions to eq 2. Only one solution, however, minimizes the free energy. In Figure 1b, the liquid phase in equilibrium with the crystal lies to the right of the liquid two-phase region, while in Figure 1d, it has moved to the left, with the result that the lowest free energy state no longer involves liquid–liquid equilibrium. At one particular temperature, T_3, a three-phase point emerges, where polymer crystal is in equilibrium with two distinct liquid phases; this point is the monotectic.[17]

Figure 1e shows the phase diagram resulting from the above constructions. Within the two-phase region, the crystal saturation curve exhibits a van der Waals like loop. Below T_3, the binodal curve has no equilibrium significance, since crystallization is now the thermodynamically preferred phase transformation. Still, the shape of the ΔG_m vs concentration curve in Figure 1d indicates that liquid–liquid demixing may still play a role in determining the resulting morphology.[17] Clearly, the composition region between the two inflection points will be completely unstable, and spinodal decomposition is expected to precede crystallization, which requires formation of a stable nucleus. Similarly, in the metastable region between the dilute branches of the spinodal and binodal curves, it would be impossible to form a stable nucleus for crystallization without first nucleating growth of a concentrated, metastable liquid phase. Thus, although below T_3 crystal–liquid equilibrium is predicted, liquid–liquid phase separation can still play an important role in governing the crystal morphology due to kinetic factors. These conclusions have been born out in observed phase-separated morphologies.[12,14,15]

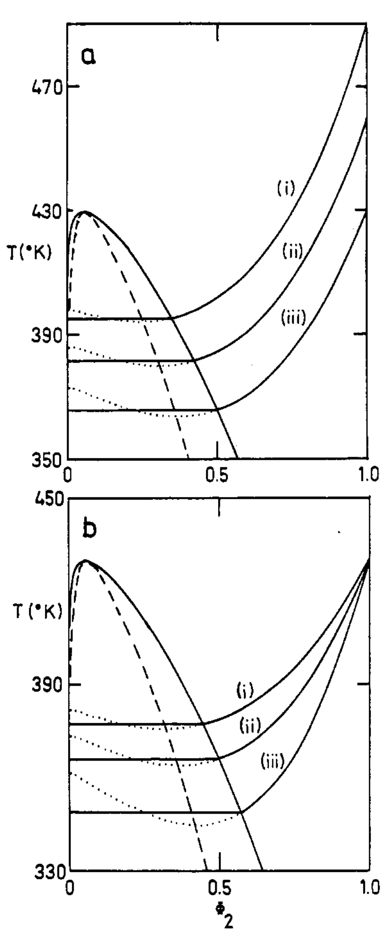

Figure 2. Effect of crystal parameters on phase diagram. $\chi = -0.7 + 541.5/T$, $r = 300$. (a) Effect of T_m^0: ΔH_u = 1500 cal/mol, T_m^0 = (i) 490, (ii) 460, (iii) 430 K. (b) Effect of ΔH_u: T_m^0 = 430 K, ΔH_u = (i) 2000, (ii) 1500, (iii) 1000 cal/mol.

Results and Discussion

Polymer Solutions. A. Effect of Crystal Parameters. The liquid–liquid binodal curve for a polymer solution with $r = 300$ was calculated with the aid of the subroutine ZSPOW from the IMSL math library. The equilibrium crystal saturation curve, given by eq 3a, may then be superimposed upon the liquid-phase diagram, as shown in Figure 2. The temperature dependence of χ was taken from typical values for polypropylene solutions,[11] while the various crystal parameters cover what may be considered a typical range.[5] As shown in Figure 2a, changing the equilibrium melting temperature of the polymer basically shifts the entire crystal saturation curve, where as Figure 2b shows that the enthalpy of fusion controls the slope of the curve. Within the liquid binodal curve, the van der Waals type loop is shown as a dotted line, to emphasize that eq 3a is not valid in this region of the phase diagram. Although not discernible on these phase diagrams, the crystal melting curve does in fact turn back down in extremely dilute solutions and emerge on the dilute side of the binodal for temperatures below the three-phase point, as shown schematically in Figure 1e. Before entering the two-phase region, the crystal melting curve exhibits positive curvature for all of these parameters. While such behavior has been observed,[7] it is more common in these systems to observe very little, and usually negative, curvature.[10,11,6] This is either a consequence of concentration dependence of the interaction parameter, or the fact that crystallization or melting of polymers generally are not in equilibrium when they are observed. Thus, we do not expect to find detailed experimental agreement with the predicted equilibrium phase diagram. Still, the general form of the phase diagrams is in line with published observations.

The crystal melting point equation is generally given in a much simpler form[3] than we have used, by ignoring terms which are divided by r and assuming a constant value for χ. When these assumptions are used, the calculated melting curves are remarkably similar to those shown in Figure 2, with discrepancies of less than about 3 K over most of the composition range. Thus, it would seem that the phase diagram is insensitive to the temperature dependence of χ as well as those terms divided by r. In the extremely dilute case, however, the melting curve does not turn back down, and consequently, it does not exit the binodal at even close to the correct point. This is because not all terms are small compared to r as Φ_2 approaches 0. In addition, in order to form the complete phase diagram, it is necessary to superimpose solutions to eq 1 and 2, and any simplifying assumptions must be taken into account equally in both cases. Thus, although the simplified relation may give very nearly the correct results, the complete crystal melting equation given in eq 3a must be used for calculation of consistent equilibrium phase diagrams.

B. Effect of χ. Figure 3 shows the effect changing the magnitude of χ has on the monotectic phase diagram structure. In these phase diagrams, solid lines represent equilibrium phase boundaries, while the broken lines represent nonequilibrium boundaries that may still affect the phase separation process. Also, the van der Waals loops have been removed for clarity. As the unfavorable enthalpic terms decrease in importance, the size of the liquid–liquid two-phase region decreases, until the crystal melting curve no longer intersects the binodal, and crystal–liquid equilibrium is predicted everywhere in the phase diagram. One striking feature of these phase diagrams is the relative constancy of the crystal melting curve despite the wide range of interaction parameters used. For example, at $\Phi_2 = 0.8$, the polymer melting temperature changes only by 3 K from Figure 3a to 3c, despite the very large change in solvent quality manifested in the gross changes in the position of the binodal curve. As in the previous section, we note that details of the interaction parameter have little effect on the crystal melting point depression over much of the phase diagram. This prediction is born out well in experimental observations, where despite extreme changes in the relative importance of liquid–liquid phase separation the crystal melting curve never changes dramatically.[6,7,10,11]

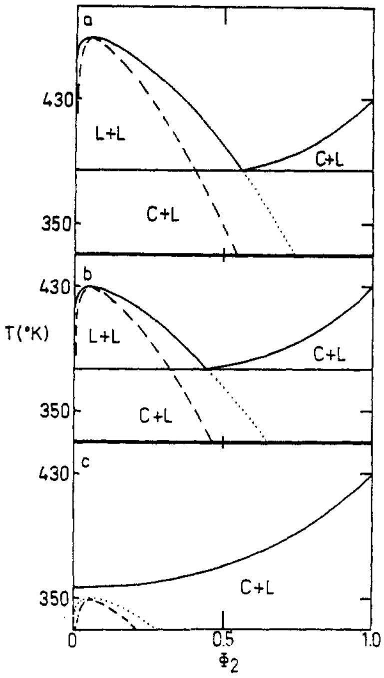

Figure 3. Effect of interaction parameter on phase diagram. T_m^0 = 430 K, ΔH_u = 2000 cal/mol, r = 300. (a) $\chi = -0.7 + 591.9/T$. (b) $\chi = -0.7 + 541.5/T$. (c) $\chi = -0.7 + 440.8/T$.

Although the binodal curve has no equilibrium significance below the three-phase point, liquid–liquid phase separation may still play a role in governing the resulting morphology, despite the fact that crystallization is the equilibrium phase transformation. Due to the high nucleation barrier to polymer crystallization, formation of a stable crystal nucleus may be preceded by liquid demixing. Furthermore, as discussed earlier, in certain portions of the diagram crystallization would necessarily be preceded by liquid phase separation.[17] Even in the case of Figure 3c, where liquid–liquid equilibrium is *never* predicted, it is conceivable that by a rapid enough temperature quench the region of liquid instability could be reached prior to crystal nucleation, with the consequence that liquid–liquid phase separation would play a major role in determining the resulting crystal morphology. Schaaf et al. have attributed certain globule-like morphologies to crystallization from poor solvents in which liquid–liquid phase separation plays a role in the equilibrium phase diagram;[12] however, it should be possible to find a solvent just good enough to realize a phase diagram of the type in Figure 3c and allow such morphologies to be produced, even though no equilibrium liquid two-phase region exists.

In a related topic, McHugh and co-workers have observed that flow-induced crystallization of polyethylene from dilute xylene solutions is preceded by a liquid-like phase separation forming a concentrated amorphous phase, which is subsequently transformed into an oriented fiber.[18] It is hypothesized that deformation of polymer chains effectively shifts the binodal to higher temperatures, allowing liquid–liquid phase separation to occur, which may be predicted from a thermodynamic analysis of flow-induced phase separation.[19] These predictions are also in line with observations by Malkin et al., who studied the effect of deformation on a monotectic polymer system.[20] From these considerations, we see that the interaction of liquid–liquid demixing and crystallization may play an important role in a variety of phase separation phenomena.

C. Crystallizable Solvent. Thus far in the discussion, the possibility of solvent crystallization has been ignored. Usually, the low molecular weight diluent will crystallize at a temperature sufficiently low so that essentially all of the polymer is in a pure crystalline phase.[21] However, if

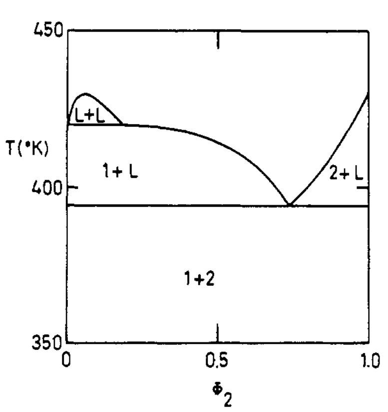

Figure 4. Phase diagram with solvent crystallization. $\chi = -0.7 + 541.5/T$, $r = 300$, $T_m{}^0 = 430$ K, $T_{m,1}{}^0 = 420$ K, $\Delta H_u = 2000$ cal/mol, $\Delta H_{f,1} = 3000$ cal/mol.

the solvent melting temperature is sufficiently high, then a eutectic will form at an intermediate concentration, and it is necessary to describe the melting point depression of both the polymer and the solvent. Such eutectic phase diagrams have been observed for solutions of polyethylene,[21,22] polypropylene,[23] polyethylene oxide,[24] and poly(ϵ-caprolactone),[25] and the construction of the equilibrium phase diagrams is well understood.[21] Eutectic solidification is another example of how phase separation may be used to control the morphology of polymers. For example, Smith and Pennings were able to form chain-oriented crystals of polyethylene by crystallizing at the eutectic composition.[22] The description of the melting point depression of the diluent parallels exactly that given above for the polymer, with the resulting expression

$$\frac{1}{T_{m,1}} = \left[1 + \frac{R\beta\Phi_2{}^2}{\Delta H_{f,1}{}^0}\right]^{-1}\left[\frac{1}{T_{m,1}} - \frac{R}{\Delta H_{f,1}{}^0}\left[\left(1 - \frac{1}{r}\right)\Phi_2 + \ln\left(1 - \Phi_2\right) + \alpha\Phi_2{}^2\right]\right] \quad (4)$$

for the melting temperature of the diluent in the presence of a polymer solution with polymer volume fraction Φ_2. The phase diagram is constructed by extending the melting point depression curves of the polymer and solvent until they intersect, giving the eutectic point.

There is, of course, no reason to restrict consideration to crystallizable diluents that are good solvents, and the effects of liquid–liquid immiscibility may be taken into account in this case as well. Since the binodal is shifted dramatically toward the pure solvent axis, in most cases it is expected that the monotectic phase reaction will involve the crystalline solvent rather than polymer. An example of such a phase diagram is given in Figure 4. Here 1 denotes pure crystalline solvent, while 2 denotes crystalline polymer. In this case, the monotectic occurs in a dilute solution when the solvent melting depression curve intersects the binodal. This temperature is a three-phase point, where solvent crystal is in equilibrium with two liquid phases. Below this temperature, the phase diagram takes on the characteristic form of a eutectic.[21] Below the eutectic temperature, the pure phases of crystalline solvent and polymer coexist. Although this equilibrium phase diagram is relatively simple, the possibilities afforded by liquid demixing and monotectic and eutectic crystallization would allow a large variety of morphologies to be realized, depending on thermal history. To date, this more complicated phase structure has not been observed experimentally; however, given the variety of systems that exhibit the monotectic or eutectic phase diagram, it should not be too difficult to determine an appropriate polymer–solvent pair that would exhibit this kind of phase diagram.

Binary Blends. The study of crystallization in blends has been limited almost exclusively to miscible blends in which one component is crystallizable. Studying the melting point depression as a function of composition has been used to determine the interaction parameter in blends of isotactic polystyrene with PPO[26–28] as well as with other polymers[28] and of poly(vinylidene fluoride) blended with PMMA[29] and PEMA,[30] to give but a sampling of the many studies in this area. In at least one study, miscible blends of *two* crystallizable polymers have been studied.[31] Unlike the case of solution crystallization, the melting point depression in a blend varies very strongly with the interaction parameter, since for most miscible blends the term containing χ in eq 3b dominates for large r. In order to get appreciable melting point depression, χ has to be negative, which is also the general requirement for formation of miscible blends. If χ becomes only slightly positive, a liquid–liquid two-phase region results, and, from eq 3b, only the slightest melting point depression is expected.

Crystallization in binary blends with limited liquid miscibility has recently been studied for two systems.[13,14,15] Inaba and co-workers demonstrated that a fine degree of control of the blend morphology may be achieved through the interplay of crystallization and spinodal decomposition,[14,15] while Tanaka and Nishi have also demonstrated the unusual phenomenon of liquid-phase separation induced ahead of a crystal growth front in such a blend.[13] In both studies, however, only schematic phase diagrams are presented. In one case, no attempt is made to represent the crystal saturation curve at all,[14] while in the other the crystal saturation is not shown to execute any sort of van der Waals loop within the two-phase region;[13] in neither of these schematic phase diagrams is there any indication that a three-phase point emerges.

In this paper, typical phase diagrams have been calculated for symmetric binary blends exhibiting the three usual liquid–liquid phase structures: upper critical solution temperature (UCST), lower critical solution temperature (LCST), and hour glass. The form of the phase diagram was achieved by assuming a temperature dependence of χ empirically to give the desired shape. While such an approach is not rigorous, it is reasonable to hope for qualitative agreement with the results for more sophisticated solution models.[1] The results of these calculations are presented in Figure 5. In this case, there is negligible depression of the polymer melting point over most of the composition range, with only slight depression occurring as Φ_2 tends toward 0. The small magnitude of the depression may be highlighted by noting that the three-phase point is no lower than 429.9 K for any of the three given phase diagrams, a depression of at most 0.1 K. Thus, the crystal melting temperature in this case is essentially invariant with respect to composition. It should be noted that although Tanaka and Nishi observed melting point depression,[13] this is primarily a consequence of the extremely low molecular weight of the amorphous component in their blend; in the case of a blend of two high molecular weight components, negligible depression is expected. Unlike the case with the solution, one cannot even approximate eq 3b by throwing out the term divided by r when positive values of χ are considered, as melting point *elevation* is then predicted, which of course is nonphysical. It is only the small effect of the logarithmic term which allows for melting point depression.

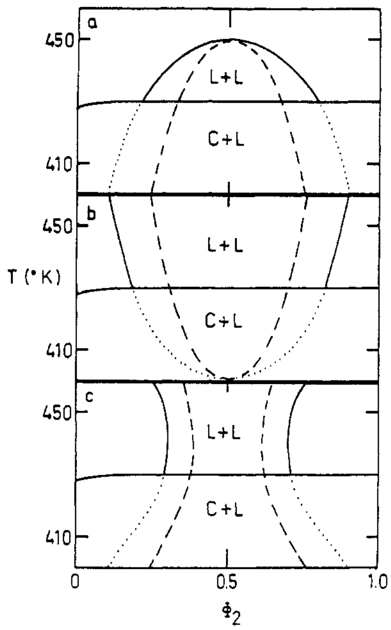

Figure 5. Phase diagrams for symmetric blends with various forms of liquid two-phase region. $T_m{}^0 = 430$ K, $\Delta H_u = 2000$ cal/mol, $r = 300$. (a) UCST: $\chi = -0.01324 + 8.958/T$. (b) LCST: $\chi = -0.00992 + 4.147 \times 10^{-5}T$. (c) Hour glass: $\chi = 0.00706 + 8.272 \times 10^{-8}|T - 440|^3$.

The extremely small melting point depression in these phase diagrams is a reflection of the fact that very subtle free energy effects dominate the liquid-phase diagram for immiscible blends. Since this would also be the case even if a more realistic solution model were used,[1] the ad hoc approached used above may be justified. Similarly, it is clear that asymmetry in the blend molecular weights would have a negligible effect on the basic nature of the crystal saturation curve and the small magnitude of the melting point depression.

Parts b and c of Figure 5 are particularly interesting in that at intermediate concentrations there is no temperature at which a one-phase system can exist at equilibrium. This is cause for some concern in the work of Inaba, in that the initial conditions of their blends are at best ill-defined, particularly in that they are cast from a solution, so that a corresponding ternary phase diagram would be required to form some analysis of the possible phase transformations which may occur during sample preparation.[14] From consideration of these equilibrium phase diagrams, it is clear that the analysis of crystallization from immiscible blends would be complicated by the uncertainty regarding the initial condition; however, the results of Inaba et al. do indicate that control of the relative rates of crystallization and phase separation does allow for a wide range of crystal domain structures.[15]

Conclusions

In this paper phase diagrams have been calculated for binary polymer systems in which both crystallization and liquid–liquid phase separation are possible. The form of the diagrams is in good agreement with experimental observations on solutions which exhibit the monotectic phase diagram, as are certain predictions, such as the relative invariance of the crystal melting curve at high polymer concentrations, despite substantial changes in the size of the liquid two-phase region. Several predictions of this analysis may be investigated by future experimentation: (i) Even when no liquid phase separation occurs in the equilibrium phase diagram, the shape of the free energy of mixing curve as well as kinetic limitations of polymer crystallization dictates that liquid–liquid demixing may still play a role in determining the morphology of crystallization from solutions in marginally good solvents. (ii) A phase diagram incorporating both monotectic and eutectic phase structures should be obtainable in polymer solutions in poor solvents with high melting points.

Negligible melting point depression is predicted in immiscible binary blends. Consideration of the equilibrium phase diagrams for these blends indicates that care must be taken to define the initial state of the blend in studies of phase separation and crystallization in these more complicated systems. In particular, when samples are formed by casting blends from solutions, ternary phase diagrams are required to give some indication of the thermodynamic state of the initial blend.

Acknowledgment. I thank C. W. Frank for helpful suggestions and encouragement and A. J. McHugh for valuable discussions.

References and Notes

(1) Olabisi, O.; Robeson, L. M.; Shaw, M. T. *Polymer-Polymer Miscibility*; Academic Press: New York, 1979.
(2) Kesting, R. E. *Synthetic Polymeric Membranes*; Wiley: New York, 1985.
(3) Flory, P. J. *Principles of Polymer Chemistry*; Cornell University Press: Ithaca, NY, 1953.
(4) Tompa, H. *Polymer Solutions*; Butterworths: London, 1956.
(5) Mandelkern, L. *Crystallization of Polymers*; McGraw-Hill: New York, 1964.
(6) Richards, R. B. *Trans. Faraday Soc.* **1946**, *42*, 10.
(7) Flory, P. J.; Mandelkern, L.; Hall, H. K. *J. Am. Chem. Soc.* **1951**, *73*, 2532.
(8) Bueche, A. M. *J. Am. Chem. Soc.* **1952**, *74*, 65.
(9) Quinn, F. A.; Mandelkern, L. *J. Am. Chem. Soc.* **1958**, *80*, 3178.
(10) Nakajima, A.; Fujiwara, H.; Hamada, F. *J. Polym. Sci., Polym. Phys. Ed.* **1966**, *4*, 507.
(11) Nakajima, A.; Fujiwara, H. *J. Polym. Sci., Polym. Phys. Ed.* **1968**, *6*, 723.
(12) Schaaf, P.; Lotz, B.; Wittmann, J. C. *Polymer* **1987**, *28*, 193.
(13) Tanaka, H.; Nishi, T. *Phys. Rev. Lett.* **1985**, *55*, 1102.
(14) Inaba, N.; Sato, K.; Suzuki, S.; Hashimoto, T. *Macromolecules* **1986**, *19*, 1690.
(15) Inaba, N.; Yamada, T.; Suzuki, S.; Hashimoto, T. *Macromolecules* **1988**, *21*, 407.
(16) Burghardt, W. R.; Yilmaz, L.; McHugh, A. J. *Polymer* **1987**, *28*, 2085.
(17) Cahn, J. W. *J. Am. Ceram. Soc.* **1969**, *52*, 118.
(18) Rietveld, J.; McHugh, A. J. *J. Polym. Sci., Polym. Phys. Ed.* **1985**, *23*, 2339.
(19) McHugh, A. J.; Vrahopoulou, E. *Macromolecules* **1984**, *17*, 2657.
(20) Malkin, A. Y.; Kulichikhin, S. G.; Chalykh, A. E. *Polymer* **1981**, *22*, 1373.
(21) Smith, P.; Pennings, A. J. *Polymer* **1974**, *15*, 413.
(22) Smith, P.; Pennings, A. J. *J. Mater. Sci.* **1976**, *11*, 1450.
(23) Smith, P.; Pennings, A. J. *J. Polym. Sci., Polym. Phys. Ed.* **1977**, *15*, 523.
(24) Gryte, C. C.; Berghmanns, H.; Smets, G. *J. Polym. Sci., Polym. Phys. Ed.* **1979**, *17*, 1295.
(25) Wittmann, J. C.; Manley, R. St. John *J. Polym. Sci., Polym. Phys. Ed.* **1977**, *15*, 1089.
(26) Berghmanns, H.; Overbergh, N. *J. Polym. Sci., Polym. Phys. Ed.* **1977**, *15*, 1757.
(27) Kwei, T. K.; Frisch, H. L. *Macromolecules* **1978**, *11*, 1267.
(28) Runt, J. P. *Macromolecules* **1981**, *14*, 420.
(29) Nishi, T.; Wang, T. T. *Macromolecules* **1975**, *8*, 909.
(30) Kwei, T. K.; Patterson, G. D.; Wang, T. T. *Macromolecules* **1976**, *9*, 780.
(31) Zhang, H.; Prud'homme, R. E. *J. Polym. Sci., Part B: Polym. Phys.* **1987**, *24*, 723.